Proceedings of 14th IOE Graduate Conference
Peer Reviewed
Year: 2023 Month: December Volume: 14
ISSN: 2350-8914 (Online), 2350-8906 (Print)

Multi-Hazard Map of Gulmidarbar Rural Municipality, Gulmi

Sundar Tandan [a], Basanta Raj Adhikari [b], Akhilesh Kumar Karna [c]

[a, b, c] *Department of Civil Engineering, Pulchowk Campus, IOE, TU, Nepal*

[a] sundartandan02@gmail.com, [b] bradhikari@ioe.edu.np, [c] akhileshkk@gmail.com

Abstract

Many areas of Nepal are susceptible to different types of natural disasters. For a multihazard map to be effective, each hazard must be analyzed separately and integrated. This paper generated the multi-hazard map of the Gulmidarbar Rural Municipality from the integration of the four individual hazards (landslides, forest fire, floods, and earthquakes) using the Analytical Hierarchy Process (AHP). The landslides and the forest fire maps were prepared from the frequency ratio (FR) method and the rain-on-grid method was used for the flood map preparation. The earthquake map was prepared from the seismic zoning map of Nepal which is based on the NBC:2020. These individual hazard maps were validated using different techniques and methods before the preparation of a multi-hazard map. Lastly, the merging of the separate hazard maps (landslides, forest fires, floods, and earthquakes) resulted in a multi-hazard map of the research area. From the multi-hazard map, it is seen that 12.04 percent lies at very low, 27.53 percent at low, 28.12 percent at medium, 20.69 percent high, and 11.63 percent at very high hazard levels. This multi-hazard map helps the decision-makers, urban planners, emergency responders, and policymakers with actionable insights to allocate resources efficiently, enhance preparedness, and mitigate the adverse effects of these hazards for the development of a better plan for the study area.

Keywords

landslide, forest fire, flood, earthquake, multi-hazard, QGIS

1. Introduction

Nepal is subject to a multitude of natural disasters that have catastrophic effects on the built environment and infrastructure, killing people and destroying property [1]. The most damaging natural disasters that cause fatalities and significant financial damage in Nepal include fires, earthquakes, landslides, and floods [2]. Studies on the danger of natural hazards usually focus on the effects of a single hazard, like landslides [3], floods [4], earthquakes [5], or forest fires [6].

A variety of barriers prevent multi-hazard planning: the lack of extensive data [7], the difficulty of integrating individual hazard maps [8], and the difficulty of producing geographically specific conditions and results for hazards [9]. Therefore, a lot of research is restricted to a single natural hazard, has different methods, and covers a small area, making it difficult for decision-makers to identify areas that are vulnerable to many hazards and put precautions in place [10].

Although there are many challenges in the preparation of a multi-hazard map, it has many benefits. Because the pre-disaster context can either emphasize or lessen the effects of an individual hazard, a multi-hazard strategy that considers the geographical, demographic, and physical contexts and their numerous linkages and feedbacks could significantly contribute to reducing human and financial losses [11].

Gulmidarbar Rural Municipality of Gulmi district is vulnerable to various hazards (DAO, Gulmi) that cause damage to the infrastructures and built environment every year. This paper performs the multi-hazard assessment of the Gulmidarbar Rural Municipality from the individual hazard maps. This map aids in identifying the places that are vulnerable to both single and multiple hazards, which helps planners, emergency responders, policymakers, and decision-makers create better plans by effectively allocating resources.

The study's research questions are:

1. Which factor is the most crucial in triggering landslides and forest fires in the study area?
2. Which hazard has the maximum impact in the study area?

2. Materials and Methods

2.1 Study Area

The Gulmidarbar Rural Municipality in the Gulmi district of Lumbini Province is the study area. The rural municipality is located at 27° 55' 14" N- 28° 07' 00" N to 83° 16' 30" E - 83° 22' 45" E. The Rural Municipality (RM) borders Chandrakot Rural Municipality and Chhatrakot Rural Municipality in the East, Chhatrakot Rural Municipality and Arghakhanchi in the South, Resunga Municipality in the West, Musikot Municipality and Chandrakot Rural Municipality in the North. This rural municipality has a total size of 79.99km^2 with 19,296 people living there as per the 2078 Census. It is divided into 7 wards and the headquarters of this rural municipality is located at Gaundakot.

Due to an increasing number of unplanned road constructions and unmanaged urbanization, the regional environment of this rural municipality is changing swiftly making this municipality vulnerable to natural hazards.

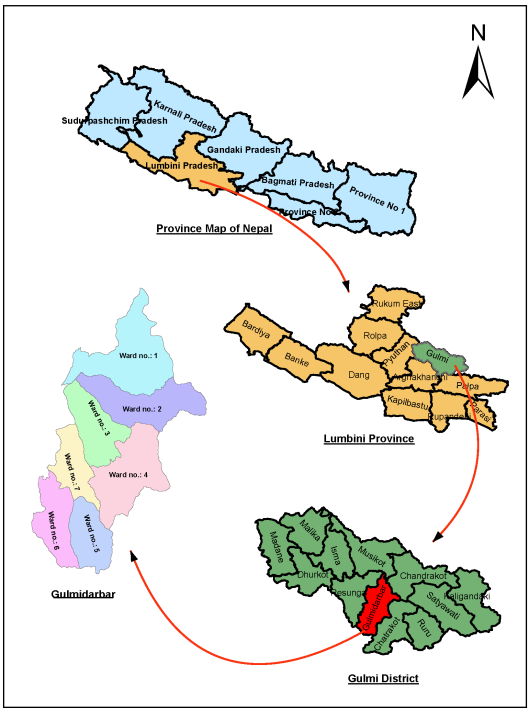

Figure 1: Map of study area

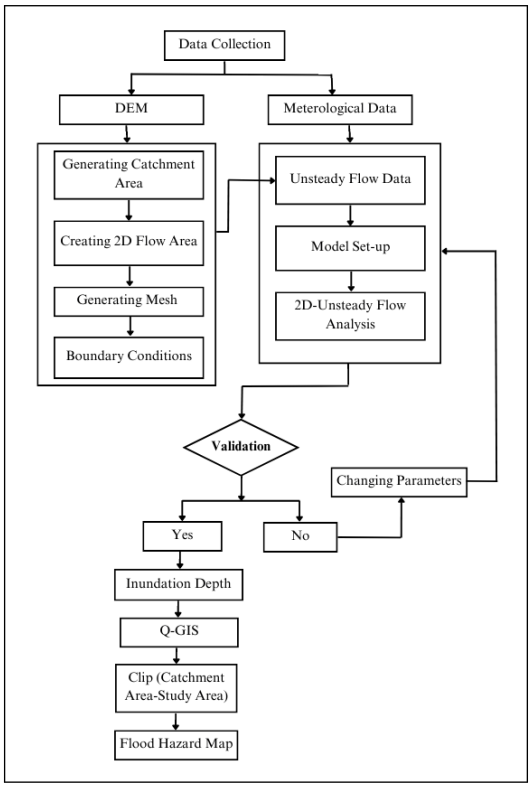

Figure 2: Methodology for preparation of Flood Hazard Map

2.2 Individual Hazard Mapping

Individual hazard mapping serves as the primary prerequisite for multi-hazard mapping. The individual hazards such as floods, earthquakes, landslides, and fires are considered in that area.

2.3 Flood Hazard Mapping

Policymakers can accurately predict and identify areas that are vulnerable to floods due to advancements in the approach and outcome capabilities of flood hazard mapping (FHM) [12]. The following factors that affect the flood are:

- **Discharge**: The excessive discharge at the stream extends its channel by overtopping its banks and flooding the low-lying areas around it [13].
- **Rainfall**: An increase in rainfall causes more ability of water to absorb which causes the rainfall-induced flood [13].
- **Landcover**: The land such as a wetland, impervious surface (pavement), barren land may reduce rainfall penetration and increase surface runoff. [14].
- **Inundation Depth**: An increase in the inundation depth increases the intensity of flooding [15].

The flood hazards map in this study was created using the Rain-on-grid approach due to its flexibility, rainfall-runoff modeling, spatially distributed representation, and data integration. The methodology for the preparation of the flood hazard map is shown in Figure 2.

The catchment area was generated from the spatial analysis in QGIS with outlet coordinates. The catchment from the aforementioned technique was imported into RAS Mapper to generate the landscape after a new project was formed in HEC-RAS. The terrain was used to extract topographical features of the 2D flow area. Mesh sizes of $100m \times 100m$ were created inside the 2D flow area. The boundary condition was set inlet by the daily rainfall data (mm) and outlet by the energy gradient 0.0015. For the unsteady model run, a plan was created from the unsteady flow data with the different computation time steps, the flood hazard map was checked and finally, the model was computed.

2.4 Landslide Susceptibility Mapping

It is the probability that the landslide would occur in a particular place due to the specific topography of the area. A number of geological, topographic, and other key parameters connected individually and in combination with the occurrence of landslides are chosen.

2.5 Forest Fire Susceptibility Mapping

The frequency of forest fires is rising worldwide, with the majority of the major accidents occurring in Asia [16]. A number of geological, topographic, and other important factors associated individually and in combination with the occurrence of forest fires are selected based on a review of the literature review.

2.6 Influencing Factors in Landslide and Forest Fire Susceptibility Mapping

Based on the literature review the influence factors for the forest fire and landslide are described in the following sections.

2.6.1 Inventory

The inventory map was created by using the previous reports, aerial photograph interpretation, and various types of field surveys. An inventory of landslides was prepared for this study using Google Earth Pro and a total number of 25 inventory landslides were recorded for the last 15 years. The inventory for the forest fire was obtained from the MODIS data and the 20 years of point data was obtained which was then changed into the raster data using QGIS.

2.6.2 Aspect

Aspect, or slope orientation, influences exposure to wind, sunlight, and precipitation; as a result, it indirectly influences other elements like soil moisture, vegetation cover, and soil thickness that are known to cause landslides and forest fires [17]. Based on DEM data, the aspect map of the study area was created and classified into nine groups, namely Flat (-1°-0°), North (0°-22.5° and 337.5°-360°), North-East (22.5°-67.5°), East (67.5°-112.5°), South-East (112.5°-157.5°), South (157.5°-202.5°), South-West (202.5°-247.5°), West (247.5°-292.5°), and North-West (292.5°-337.5°).

2.6.3 Slope

The area's morphological structure, rainfall and sunshine levels, drying winds, and hydrological processes including evapotranspiration, weathering, vegetation, and plant root growth are all influenced by slope and contribute to the many risks in the area (landslide, forest fire, and floods) [18]. DEM data were used to prepare the map of the slope. It is divided into five groups; 0-15°, 15°-30°, 30°-50°, 50°-70°, and 70°-90°.

2.6.4 Landuse and Landcover

The frequency of unstable slopes is increased by specific land use and land cover changes (LUCCs), such as deforestation, steep slopes, and slope ruptures caused by road building [19], i.e., Increases the likelihood of different dangers occurring and can have a significant effect on them [20]. The land use map prepared by ICIMOD was used in this study after resampling from 30m resolution to 12.5 m resolution.

2.6.5 Curvature

The driving and resistive forces in the direction of mass flow are influenced by curvature. Three classes were identified in the curvature map, which was produced using the DEM: convex (positive), flat (zero), and concave (negative).

2.6.6 Distance from drainage and road

Because several drainage networks erode the slope base and saturate the underwater portion of the slope-forming material, rivers with multiple drainage networks are more likely to experience landslides and floods [21]. The stream map was generated by using the buffer tool in QGIS and was classified as subclasses-<50, 50-<150, 150-<500, and >500 m.

Depending on its position in the environment, a road segment can function as a barrier, a net source, a net sink, or a corridor for water movement. As a result, it is usually a source of hazards [22]. The road layer was extracted from the OpenStreetMap using the QUickOSM plugin and distance from the road was developed using the buffer tool and was classified as subclasses: <300, 300-<500, and >500 m.

2.6.7 NDVI and NDMI

The vegetation cover often has a great influence on natural hazard occurrence as they are related to anthropogenic interference on the hill slopes(B. Pradhan and Lee, 2009). NDVI was generated from the Landsat-8 satellite image by using the formula: NDVI=(NIR-R)/(NIR+R) Where NIR-spectral reflectance of near-infrared bands and R-spectral reflectance of red bands. It was classified into subclasses:<0.14,0.14-<0.22,0.22-<0.27,0.27-<0.31,0.31-<0.36,and>0.36.

NDMI (Normalized Difference Moisture Index) is a vegetation index commonly used to detect moisture content in vegetation. It was generated from the Landsat-8 satellite using the formula: NDMI = (NIR - MIR) / (NIR + MIR) where NIR is the reflectance value in the near-infrared band (Band 8A), and MIR is the reflectance value in the mid-infrared band (Band 11).It was classified into subclasses: <0.1,0.1-<0.2,0.2<0.3 and >0.3.

2.6.8 Elevation and Relative Relief

Elevation is one of the elements influencing natural hazards because it influences temperature, humidity, precipitation, and vegetation, among other environmental conditions [23]. The elevation map was derived from DEM and was classified as <1000, 1000-<1500, and >1500 m.

Maps showing relative relief show the potential energy for mass movement and erosion resulting from variations in elevation within a unit area. That was categorised as <188, 188-<297, 297-<406, and >406.

2.6.9 Rainfall

Rainfall can cause hazards but ground conditions are also significant [24]. By using the Thiessen polygon the rainfall of the study area was interpolated using the stations: Tamghas (725) Bharse (733) Musikot (722) and Ridi (701) and was classified as: <2000, 2000-<2300 and >2300 mm.

2.6.10 Geology and Soil

The geology of an area governs the strength of rock and soil permeability thus; geology has an impact on hazards. The geology map produced by ICIMOD (2020) was used. Lakharpata, Galyang, Syangja, and Ranimatta formations were found in the study area.

The soil data was obtained from the ICIMOD and three types of soli data CMe (Eutric Cambisols), CMg (Gleyic Cambisols), and CMx (Chromic Cambisols) were found in the study area.

2.6.11 Distance to settlement

The majority of the urban poor live in informal settlements, which are frequently situated near natural hazards. The settlement data was obtained from the NASA firms(R_{26},C_{26}) The distance to the settlement map was obtained from the buffer tool and was categorized into four classes <1000, 1000-<2000, 2000-<3000 and >3000 m.

2.6.12 Wind Speed

By transferring heat and burning embers to fresh fuels and by directing the flames toward the unburned fuels in front of the fire, wind aids in the spread of fires. The data of the wind speed was obtained from the global wind atlas and was classified as <1,1-<1.6,1.6-<2.4,2.4-<3.2 and >3.2 m/sec.

The frequency ratio method was used in this study for the landslide and forest fire susceptibility mapping due to its simplicity, data availability, spatial analysis, comparative analysis, and interpretability. The methodology for the forest fire and the landslide susceptibility mapping is shown in Figure 3.

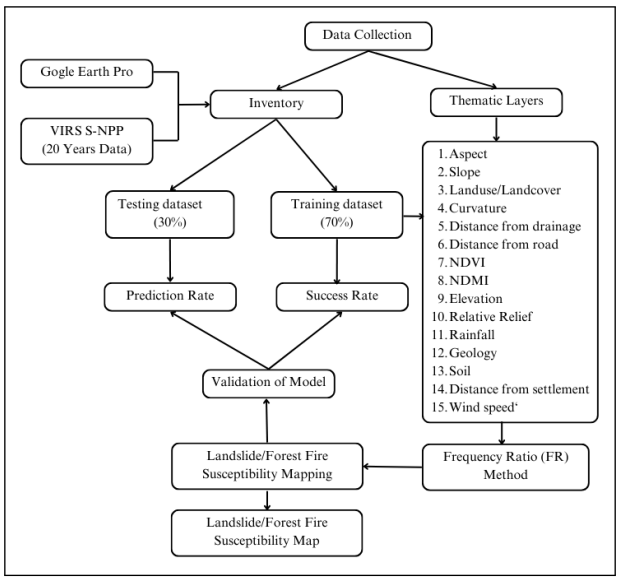

Figure 3: Methodology for preparation of Landslide/Forest Fire Susceptibility Map

2.7 Earthquake Hazard Mapping

Uncertainties in earthquake size, location, and time of occurrence can be considered probabilistic seismic hazard analysis [25]. The seismic map that was prepared by NBC:2020 was used to obtain the earthquake (seismic) zoning map of the study area. The seismic zoning map image file was inserted into QGIS and was converted to the georeferenced image with the help of georeferencing. To generate the seismic zoning map of the study area, the georeferenced image was clipped by the study area and the clipped file was classed using the NBC:2020.

2.8 Multi-Hazard Assessment

2.8.1 Determination of Hazard Weights for Preparation of Multi-Hazard Map

Analytical Hierarchy Process was used for the determination of the weight of each hazard. Saaty [26] has developed a systematic method for applying AHP to decision-making-related research. The method starts with (i) describing the issue and establishing the goal and objective; (ii) putting the objectives at the top of the hierarchy, then the intermediate levels; and (iii) organizing the objectives at the bottom level, which usually has the list of alternatives. (iii) allocating numerical values according to the proportionate weight of each factor (pairwise comparison); (iv) creating the comparison matrix; and (v) computing the normalized principal eigen vectors, which incorporate the parameter weights. On a scale of 1 to 9, where 1 represents equal relevance and 9 represents the exceptional importance of one domain over another, experts rank the important levels. Every pairwise comparison immediately assigns a reciprocal. The maximum eigenvalue, consistency ratio, consistency index, and normalized primary eigenvectors are calculated for each criterion. For obtaining the consistency index (CI) the maximum eigenvalue (λ_{max}) is used as given by the equation:

$$CI = \frac{(\lambda_{max} - n)}{(n-1)} \tag{1}$$

where n is the size of the matrix. For the AHP method, the consistency ratio (CR) which is determined by the equation below should be valid only when CR is less than 10 percent, otherwise, the matric is inconsistent and judgment should be modified to validate the realistic results [27].

$$CR = \frac{CI}{RI} \tag{2}$$

where RI is the random consistency index for various matrix orders (n).

Table 1: Table showing the calculation of the weight of each hazard.

S.No.	**Hazards**	H_1	H_2	H_3	H_4	**Weight**(W_i)
1.	Landslide (H_1)	1.00	4.00	3.00	6.00	0.549
2.	Forest Fire (H_2)	0.25	1.00	0.50	3.00	0.147
3.	Flood (H_3)	0.33	2.00	1.00	4.00	0.239
4.	Earthquake (H_4)	0.17	0.33	0.25	1.00	0.065

Table 2: Table demonstrating pairwise comparative consistency.

Causative Factors	**n**	λ_{max}	**CI**	**RI**	**CR**
	4	4.081	0.027	0.900	0.030

2.8.2 Multi-Hazard Mapping

The AHP method was used for the preparation of the multi-hazard map from the individual hazards. The individual

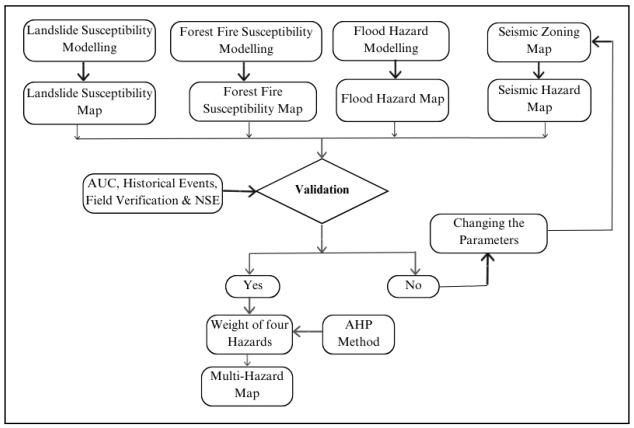

Figure 4: Methodology for preparation of multi-hazard map

hazard maps were validated and normalized by using the raster calculator before the preparation of the multi-hazard map [11]. The weights of each hazard were calculated from the AHP. Based on the weightage value the multihazard map was prepared by using Equation 3.

$$MHI = \sum_{i=1}^{n} H_i \times W_i \tag{3}$$

where n is the number of hazards, Hi is the name of an individual hazard, and Wi is the weight assigned by the AHP approach to each hazard. The methodology for the preparation of the multi-hazard map is in the form of a flowchart is shown in Figure 4.

3. Results and Discussions

3.1 Landslide Hazard Assessement

A total number of ten thematic layers and their weightage were: aspect (8%), slope (12%), geology (9%), land use (11%), curvature (9%) distance from drainage (8%), distance from the road (9%), rainfall (12%), Normalized Difference Vegetation Index (11%) and relative relief (11%) were used to identify the different degrees of susceptibility to landslide occurrence.

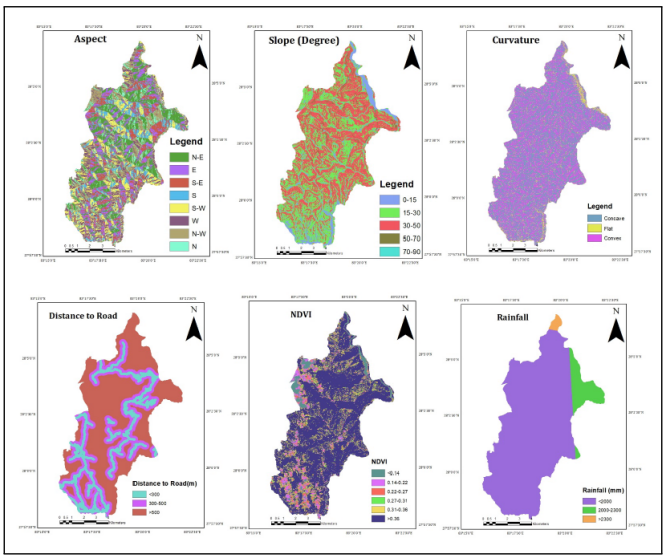

Figure 5: Thematic Map showing (a) aspect (b) slope (c) curvature (d) distance from roads (e) Normalized Difference Vegetation Index (NDVI) (f) Rainfall

The landslide susceptibility map of the study area is shown in Figure 6.

Using the Jenks Natural breaks classification method, the landslide susceptibility map was divided into five classes: very low, low, medium, high, and very high. From the landslide susceptibility map around 13.07%-very low, 20.28% low. 25.93% medium, 17.64% high, and 22.86% very-high hazard zones of the landslide. The affected area for different hazard levels is given in Table 3.

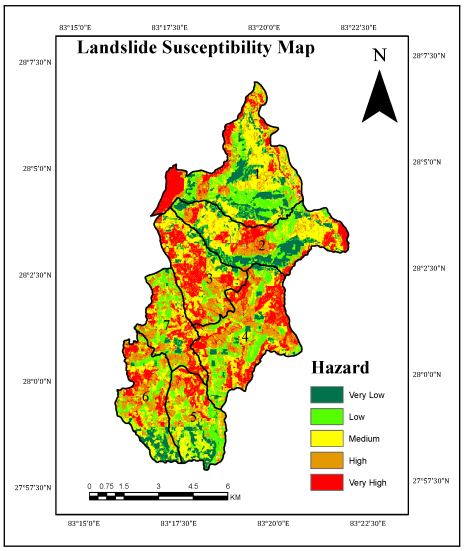

Figure 6: Landslide susceptibility map of the study area

Table 3: Table showing landslide affected area for different hazard levels

S. No.	Landslide Hazard Zone	Area	
		sq.km.	percent
1	Very Low	10.394	13.07%
2	Low	16.160	20.28%
3	Medium	20.662	25.93%
4	High	14.058	17.64%
5	Very High	18.221	22.86%

3.2 Forest Fire Hazard Assessement

A total number of eleven thematic layers and their weightage were: aspect (6%), slope (11%), topographic wetness index (9%), curvature (8%), soil (13%), distance from road (6%), distance from settlement (16%), NDVI (6%), NDMI (8%), elevation (12%), and wind speed (5%) were considered to identify the forest fire susceptibility map in the study area. Distance from settlement contributed to the maximum weight while the contribution of wind speed was lowest.

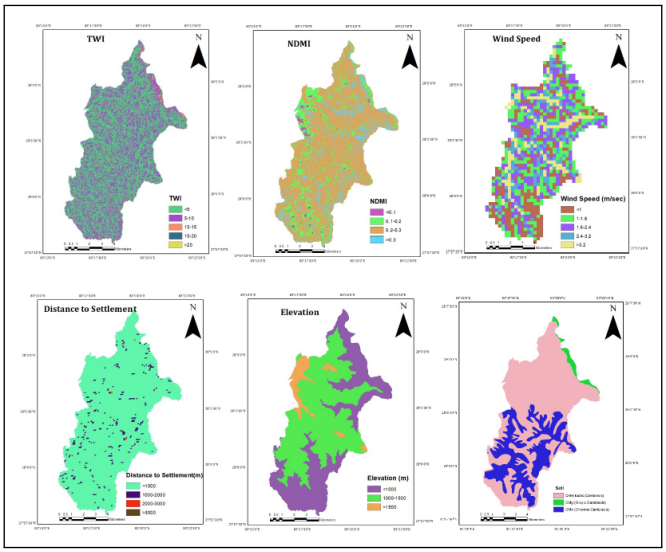

Figure 7: Thematic Map showing (g).TWI (h).NDMI; (i).Wind Speed; (j). distance from the settlement; (k). elevation; (l).soil.

Using the Jenks breaks method, the forest fire susceptibility map was divided into five classes: very low, low, medium, high, and very high. From the forest fire susceptibility map around 6.22%-very low, 26.76% low. 32.96% medium, 29.71% high, and 4.36% very-high hazard zones of the forest fire. The affected area for different hazard levels and susceptibility map of forest fire is given in Figure 8.

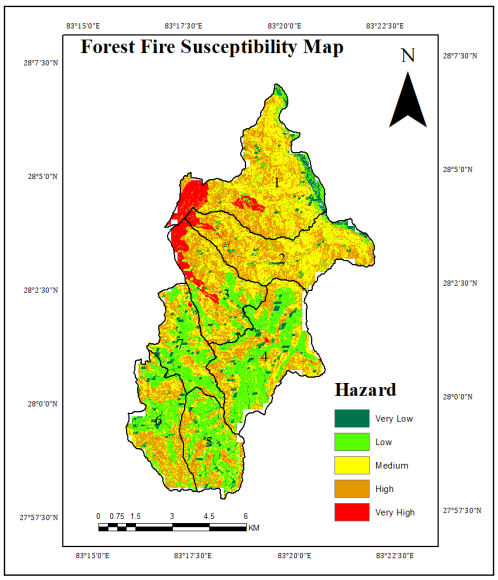

Figure 8: Forest Fire susceptibility map of study area

Table 4: Table showing forest fire affected area for different hazard levels.

S. No.	Forest Fire Hazard Zone	Area	
		sq.km.	percent
1	Very Low	4.954	6.22%
2	Low	21.327	26.76%
3	Medium	26.269	32.96%
4	High	23.675	29.71%
5	Very High	3.474	4.36%

3.3 Flood Hazard Assessement

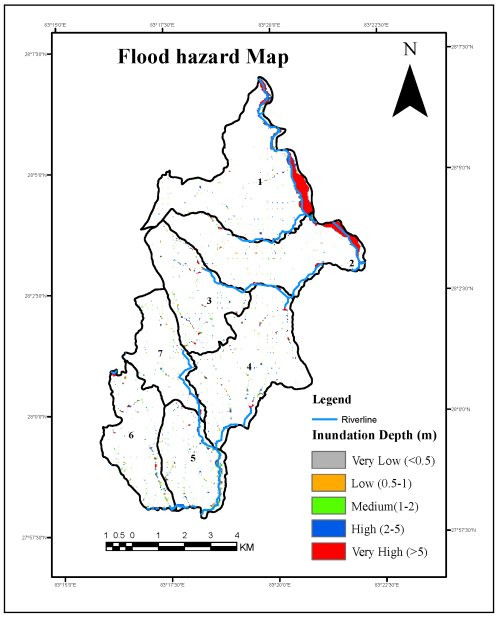

Figure 9: Flood hazard map of the study area

The flood hazard map was prepared from the HEC-RAS 2D based on the rain-on-grid method for a 100-year return period of rainfall. Based on the depth of inundation, five classes were identified on the flood hazard map [28]: very low (<0.5), low (0.5-<1), medium (1-<2), high (2-<5), and very high (>5).From the flood hazard map total area of 0.52%-very low, 0.57% low. 0.82% medium, 1.24% high and 2.60% very-high hazard zones.

Table 5: Table showing flood-affected areas for different hazard levels.

S. No.	Flood Hazard Zone (m)	Area	
		sq.km.	percent
1	Very Low (<0.5)	0.42	0.52%
2	Low (0.5-<1)	0.46	0.57%
3	Medium (1-<2)	0.65	0.82%
4	High (2-<5)	0.99	1.24%
5	Very High (>5)	2.08	2.60%

3.4 Earthquake Hazard Assessement

The seismic zoning map was prepared from NBC:2020.

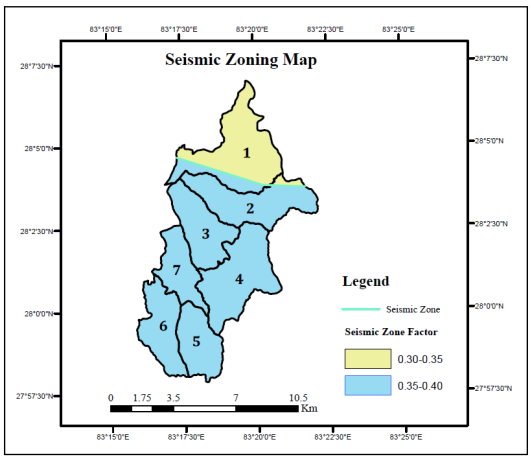

Figure 10: Seismic zoning map of the study area.

Based on the seismic zones (NBC:2020), the seismic zoning map was divided into four classes: 0-0.25, 0.25-0.3, 0.3-0.35, and 0.35-0.40. According to the map, the majority of the area (81.57%) lies at the seismic zone factor 0.35-0.40 and 18.43% of the area lies at the seismic zone factor 0.30-0.35

Table 6: Earthquake affected area for different seismic zone factors.

S. No.	Seismic Zone Factor	Area	
		sq.km.	percent
1	0.30-0.35	14.76	18.43%
2	0.35-0.40	65.30	81.57%

3.5 Multi-Hazard Assessment

After each hazard was validated and normalized, the various hazards (floods, landslides, fires, and earthquakes) were integrated and created as a multi-hazard map using the Analytical Hierarchy Process.

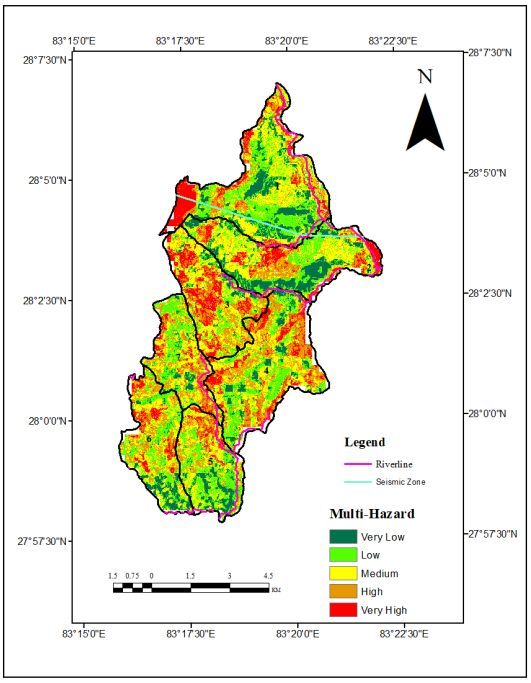

Figure 11: Multi-hazard map of the study area.

Using Natural breaks classification method, the multi-hazard map was divided into five classes: very low, low, medium, high, and very high. From the multi-hazard map, the total area of 12.04%-very low,27.53%-low, 28.12%-medium, 20.69%-high and 11.63%-very high hazard zones.

Table 7: Table showing multi-hazard affected area for different hazard levels.

S. No.	Multi-Hazard Zone	Area	
		sq.km.	percent
1	Very Low	9.58	12.04%
2	Low	21.90	27.53%
3	Medium	22.37	28.12%
4	High	16.45	20.69%
5	Very High	9.25	11.63%

3.6 Validation of the Individual Hazard Maps

The validation of the landslide hazard map was conducted by the Area under Curve (AUC) method and a field visit was conducted throughout the inventory map compilation process at Google Earth Pro. The Area Under Curve (AUC) for the landslide susceptibility map was used to calculate the success and prediction rates, which showed out to be 71.4% and 65.8% respectively.

The area under the curve (AUC) approach was utilized for verifying the forest fire hazard map. The success and the prediction rate of the model were found to be 73.8% and 66.2% respectively.

NBC:2020 generated the seismic zoning map that was applied. Since DUDBC prepared the map, validation was not needed.

The flood hazard map was calibrated and validated from the discharge data for different years by using different statistical indicators [29]: Nash-Sutcliffe efficiency (NSE), PBIAS, and Coefficient of determination (R^2).

Table 8: Stastical indicators obtained from flood hazard map

S.N	Indicators	Value	Goodness of fit
1	NSE	0.648	Good
2	PBIAS (%)	2.794	Very Good
3	R^2	0.919	Very Good

4. Conclusion

This study is focused on analyzing four significant natural hazards (landslides, floods, forest fires, and earthquakes) that have substantial impacts on a rural municipality. For each of these hazards, separate hazard maps were created for this study, and the Analytical Hierarchy Process (AHP) was then used to integrate them.

From the above analysis, it can be concluded that rainfall has the highest weightage among all causative factors for triggering landslides. Similarly, distance from the settlement is found to be the most crucial factor for forest fires.

Among the four hazards analyzed landslide has the highest impact in the study area based on the historical events that caused the highest loss and damage. To enhance the accuracy of the individual hazard mapping more variables for landslides and forest fire susceptibility mapping can be considered, the seismic zoning map based on the probabilistic seismic hazard can be created, finer mesh size 50 × 50 m and landcover map derived from NDVI can enhance the flood hazard mapping, and validation can be extended by using the different historical events.

Acknowledgments

The Department of Hydrology and Meteorology (DHM), the Government of Nepal (GoN), the International Centre for Integrated Mountain Development (ICIMOD), and the Gulmidarbar Rural Municipality are acknowledged by the authors as sources of important data and information. For their assistance with this study, the authors express their sincere gratitude to Dr. Suraj Lamichhane, Professor at IOE, Er. Ranjan Dhungel, Director, National Society for Earthquake Technology-Nepal (NSET), Er. Nirajan Devkota, Ph.D. Scholar at IOE, Anup Shrestha, Ph.D Scholar at Aalto University, Finland, and Er. Raju Aryal, Civil Engineer, Gulmidarbar Rural Municipality.

References

[1] Pradip Kumar Koirala. Disaster management institution and system in nepal. *Asian Disaster Reduction Center (ADPC), Bangkok*, 2014.

[2] Dipendra Gautam, Saraswati Thapa, Sudeep Pokhrel, and Suraj Lamichhane. Local level multi-hazard zonation of nepal. *Geomatics, Natural Hazards and Risk*, 12(1):405–423, 2021.

[3] Roberta Pellicani, Ilenia Argentiero, and Giuseppe Spilotro. Gis-based predictive models for regional-scale landslide susceptibility assessment and risk mapping along road corridors. *Geomatics, Natural Hazards and Risk*, 8(2):1012–1033, 2017.

[4] Martin Kabenge, Joshua Elaru, Hongtao Wang, and Fengting Li. Characterizing flood hazard risk in data-scarce areas, using a remote sensing and gis-based flood hazard index. *Natural hazards*, 89:1369–1387, 2017.

[5] S Dhar, AK Rai, and P Nayak. Estimation of seismic hazard in odisha by remote sensing and gis techniques. *Natural hazards*, 86:695–709, 2017.

[6] Hamed Adab, Kasturi Devi Kanniah, and Karim Solaimani. Modeling forest fire risk in the northeast of iran using remote sensing and gis techniques. *Natural hazards*, 65:1723–1743, 2013.

[7] Valentina Gallina, Silvia Torresan, Andrea Critto, Anna Sperotto, Thomas Glade, and Antonio Marcomini. A review of multi-risk methodologies for natural hazards: Consequences and challenges for a climate change impact assessment. *Journal of environmental management*, 168:123–132, 2016.

[8] Eric Tate, Susan L Cutter, and Melissa Berry. Integrated multihazard mapping. *Environment and Planning B: Planning and Design*, 37(4):646–663, 2010.

[9] Katie Johnson, Yaella Depietri, and Margaretha Breil. Multi-hazard risk assessment of two hong kong districts. *International Journal of Disaster Risk Reduction*, 19:311–323, 2016.

[10] Rajesh Khatakho, Dipendra Gautam, Komal Raj Aryal, Vishnu Prasad Pandey, Rajesh Rupakhety, Suraj Lamichhane, Yi-Chung Liu, Khameis Abdouli, Rocky Talchabhadel, Bhesh Raj Thapa, et al. Multi-hazard risk assessment of kathmandu valley, nepal. *Sustainability*, 13(10):5369, 2021.

[11] Sanam K Aksha, Lynn M Resler, Luke Juran, and Laurence W Carstensen Jr. A geospatial analysis of multi-hazard risk in dharan, nepal. *Geomatics, Natural Hazards and Risk*, 11(1):88–111, 2020.

[12] Rofiat Bunmi Mudashiru, Nuridah Sabtu, Ismail Abustan, and Waheed Balogun. Flood hazard mapping methods: A review. *Journal of hydrology*, 603:126846, 2021.

[13] Sofia Sarchani, Konstantinos Seiradakis, Paulin Coulibaly, and Ioannis Tsanis. Flood inundation mapping in an ungauged basin. *Water*, 12(6):1532, 2020.

[14] Dorcas Idowu and Wendy Zhou. Land use and land cover change assessment in the context of flood hazard in lagos state, nigeria. *Water*, 13(8):1105, 2021.

[15] Hans de MOEL and JCJH Aerts. Effect of uncertainty in land use, damage models and inundation depth on flood damage estimates. *Natural Hazards*, 58:407–425, 2011.

[16] Guido R Van Der Werf, James T Randerson, Louis Giglio, Nadine Gobron, and AJ Dolman. Climate controls on the variability of fires in the tropics and subtropics. *Global Biogeochemical Cycles*, 22(3), 2008.

[17] Aldo Clerici, Susanna Perego, Claudio Tellini, and Paolo Vescovi. A gis-based automated procedure for landslide susceptibility mapping by the conditional analysis method: the baganza valley case study (italian northern apennines). *Environmental Geology*, 50:941–961, 2006.

[18] Mirco Galli, Francesca Ardizzone, Mauro Cardinali, Fausto Guzzetti, and Paola Reichenbach. Comparing landslide inventory maps. *Geomorphology*, 94(3-4):268–289, 2008.

[19] Paola Reichenbach, C Busca, AC Mondini, and M Rossi. The influence of land use change on landslide susceptibility zonation: the briga catchment test site (messina, italy). *Environmental management*, 54:1372–1384, 2014.

[20] Santiago Beguería. Changes in land cover and shallow landslide activity: a case study in the spanish pyrenees. *Geomorphology*, 74(1-4):196–206, 2006.

[21] Aykut Akgün and Necdet Türk. Mapping erosion susceptibility by a multivariate statistical method: a case study from the ayvalık region, nw turkey. *Computers & geosciences*, 37(9):1515–1524, 2011.

[22] Biswajeet Pradhan and Saro Lee. Landslide susceptibility assessment and factor effect analysis: backpropagation artificial neural networks and their comparison with frequency ratio and bivariate logistic regression modelling. *Environmental Modelling & Software*, 25(6):747–759, 2010.

[23] Jie Dou, Hiromitsu Yamagishi, Hamid Reza Pourghasemi, Ali P Yunus, Xuan Song, Yueren Xu, and Zhongfan Zhu. An integrated artificial neural network model for the landslide susceptibility assessment of osado island, japan. *Natural Hazards*, 78:1749–1776, 2015.

[24] Junghwan Kim, Yongmin Kim, Sangseom Jeong, and Moonhyun Hong. Rainfall-induced landslides by deficit field matric suction in unsaturated soil slopes. *Environmental Earth Sciences*, 76:1–17, 2017.

[25] Hemchandra Chaulagain, Hugo Rodrigues, Vitor Silva, Enrico Spacone, and Humberto Varum. Seismic risk assessment and hazard mapping in nepal. *Natural Hazards*, 78:583–602, 2015.

[26] Thomas L Saaty et al. The analytic hierarchy process: planning, priority setting, resource allocation, 1980.

[27] Thomas L Saaty and Luis G Vargas. *Models, methods, concepts & applications of the analytic hierarchy process*, volume 175. Springer Science & Business Media, 2012.

[28] Tabarak W Mahdi, Ali N Hillo, and Ali A Abdul-Sahib. Development and classification of flood hazard map using 2d hydraulic model. In *IOP Conference Series: Materials Science and Engineering*, volume 1090, page 012122. IOP Publishing, 2021.

[29] Julio Pérez-Sánchez, Javier Senent-Aparicio, Francisco Segura-Méndez, David Pulido-Velazquez, and Raghavan Srinivasan. Evaluating hydrological models for deriving water resources in peninsular spain. *Sustainability*, 11(10):2872, 2019.